Combustion and Flame 159 (2012) 1009–1015

Contents lists available at SciVerse ScienceDirect

Combustion and Flame

journal homepage: www.elsevier.com/locate/combustflame

Experimental and numerical study of thermocouple-induced perturbations of the methane flame structure

Petr A. Skovorodko [a], Alexander G. Tereshchenko [b,*], Denis A. Knyazkov [b], Alexander A. Paletsky [b], Oleg P. Korobeinichev [b]

[a] Institute of Thermophysics, Novosibirsk 630090, Russia
[b] nstitute of Chemical Kinetics and Combustion, Novosibirsk 630090, Russia

ARTICLE INFO

Article history:
Received 30 December 2010
Received in revised form 13 May 2011
Accepted 11 October 2011
Available online 16 November 2011

Keywords:
Methane flame
Flame thermal structure
Thermocouple shape
Flame perturbation
Numerical simulation

ABSTRACT

In flame temperature measurements by a thermocouple, it is usually assumed that, due to its small size, the thermocouple produces negligible perturbations of the flame structure. Our studies show, however, that this assumption may be incorrect. The temperature of a premixed atmospheric methane/oxygen/argon flame measured by several thermocouples was found to be systematically higher than the theoretical temperature at small distances from the burner (in the region with a high temperature gradient). The external flow of the flame over a thermocouple was simulated using the full set of unsteady Navier–Stokes equations to explain the discrepancy between experimental and theoretical data. An approximate allowance for the heat release due to chemical reactions was made by adding a source term to the energy equation to provide a given temperature distribution in the unperturbed isobaric flame. The observed discrepancy was found to be related to deceleration of the flow in the vicinity of the thermocouple, resulting in additional heat release due to chemical reactions in the flow. In addition, significant additional heating of the thermocouple was observed, when it was placed in the zone with maximum concentrations of H and OH radicals.

1. Introduction

Thermocouple measurements of flame temperature profiles are widely used in experimental studies of flame structure. Flame temperature profiles allow one to evaluate the heat release in various flame zones and identify key reactions in combustion processes [1,2]. Measured temperature profiles are usually used for combustion modeling [3]; consequently measuring a flame's thermal structure with appropriate accuracy is one of the most important problems in combustion research [4]. The present paper analyzes the results of thermocouple temperature measurements near the burner. We are not aware of studies using optical methods of measuring the temperature of an atmospheric pressure flame at a distance of about 0.2 mm from the burner. At such small distances, microthermocouples are used. Flame temperature is usually measured with thermocouples of two different cross-sectional shapes (circular and rectangular or ribbon). Ribbon thermocouples are used to study the flame structure of condensed systems. Such thermocouples are made by squashing circular thermocouples, and the width of a ribbon thermocouple is 10–20 times its thickness. A detailed analysis of thermocouple measurements in flames has been given before [4–7]. Ribbon thermocouples are believed to provide improved resolution [4,8]. Radiation heat loss from thermocouples have been considered in a number of papers [5,9,10]. Experimental errors due to heat gain or heat loss from the thermocouple junction to its supports are difficult to estimate because these shoulders and the junction have different temperatures. These issues have been studied in detail by Zenin [4,11] and Heitor and Moreira [12].

It is known that to determine the actual temperature, one should take into account factors related to heat transfer between the thermocouple and its surroundings and the thermocouple's emissivity [10]. It is usually believed that uncertainty in thermocouple readings is only due to uncertainties associated with the transport properties of the gases surrounding the thermocouple and the intrinsic properties of the thermocouple as a temperature sensor, such as its shape, material, emissivity, etc. However, there may be additional sources of uncertainty in thermocouple readings, which are not reported in the literature.

In our current investigations the temperature profiles in a one-dimensional burner-stabilized premixed flame of $CH_4 + O_2 + Ar$ at atmospheric pressure were measured by a thermocouple and calculated using the PREMIX code [13] from the CHEMKIN II package. The measured temperatures near the surface of the burner (at

* Corresponding author. Address: Institute of Chemical Kinetics and Combustion, Institutskaya St. 3, Novosibirsk 630090, Russia. Fax: +7 383 330 73 50.
E-mail address: tereshag@kinetics.nsc.ru (A.G. Tereshchenko).

0010-2180/$ - see front matter © 2011 The Combustion Institute. Published by Elsevier Inc. All rights reserved.
doi:10.1016/j.combustflame.2011.10.010

distances ~0.1–0.5 mm) were systematically overestimated in comparison with the calculated ones, that may be attributed to thermocouple-induced gas-dynamic perturbations of the flow. A qualitative explanation of this may be as follows: because the gas flow is decelerated in front of the thermocouple, the velocity field near the thermocouple is subjected to perturbations. In the region with a high temperature gradient near the burner or near e.g. a solid propellant's burning surface, perturbations of the velocity field can lead to perturbations of the initial temperature field of the flame, as reflected by thermocouple readings.

The literature contains no quantitative studies of a perturbation by a thermocouple of the flow structure in a gaseous flame, in which a thermocouple is placed. It has been assumed that due to the small size of a thermocouple, any perturbations of the flame structure produced by the thermocouple are negligible. The only paper dealing with this subject is that of Fristrom and Westenberg [1], who noted that the thermocouple locally perturbs the flame's velocity profile and, actually, reflects the temperature downstream of the thermocouple. The perturbation was estimated to be about 4–5 thermocouple junction diameters. Bahlawane et al. [14] measured the temperature profile in a low-pressure ethylene flame using a thermocouple and optical techniques. From the data presented in Fig. 10b of [14], one can see that the measurements of temperature by the thermocouple are slightly higher than the optical measurements, where in the temperature gradient is appreciable. This overestimation may be due to the effect studied below, but it was not discussed previously [14].

This paper presents an experimental and numerical study of falsifications of temperatures caused by flow around thermocouples of various shapes, when placed in the region of high temperature gradients in a methane flame. The possible influence of radical recombination on the thermocouple's surface on the thermocouple measurements [10] is estimated. The problem of correcting perturbed temperature profiles requires special consideration. The results obtained are used to analyze the validity of employing thermocouples in studies of the thermal structure of flames of gaseous and condensed [15] systems.

2. Experimental technique

We studied the temperature along a one-dimensional, premixed flame of methane + oxygen + argon ($CH_4/O_2/Ar$ – 6/15/79 vol.%) stabilized on a flat burner at atmospheric pressure (Fig. 1). The flame studied is far from the limit of unstable combustion. This flame is very reproducible, in contrast to, for example, flames from condensed-system. During the experiment, the surface temperature of the water-cooled burner was kept at 368 K using a thermostat. The burner top was a porous brass disk 16 mm in diameter and 5 mm high. It was made of sintered spheres ~0.1 mm in diameter. The relative porosity of the burner disk was ~40%. The flow rate of the unburned mixture was 25 cm^3/s under standard conditions. Flow rates of the gas components of the unburned mixture were set to within ±1% by mass flow controllers (MKS Instruments Inc., Model 1259C). Reactant flow rates at the exit from the mass flow controllers were calibrated using a drum-type gas flow meter (Trommel–Gaszähler TG 05) to confirm the claimed accuracy. The burner was mounted on a translation stage so that it could be moved vertically relative to the fixed thermocouple with a positioning accuracy of 0.01 mm. The shoulders of all thermocouples were parallel to the surface of the burner. In the case of ribbon thermocouples, the broad part of the thermocouple was parallel to the burner. The distance between the burner and thermocouple was measured as that from the burner to the center of the thermocouple.

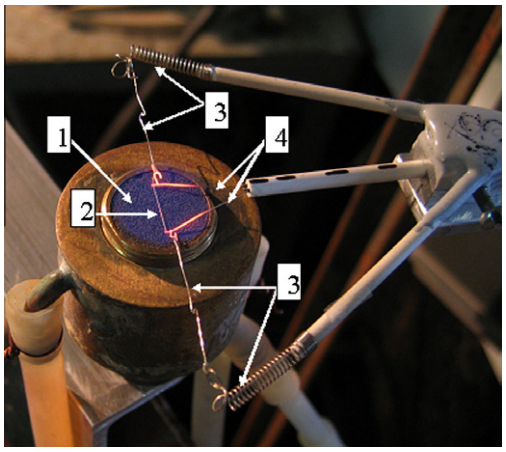

Fig. 1. A thermocouple in a flame above the burner. 1 – the burner surface, 2 – termocouple, 3 – a spring-loaded device which extends the thermocouple and compensates the thermocouple extension due to heating in the flame, 4–0.2 mm diameter leads to the thermocouple.

Temperature profiles were measured using three types of Pt/Pt + 10%Rh thermocouples coated with a thin layer of SiO_2 (~2–3 μm) to prevent catalytic processes. The process of coating the thermocouples with a thin SiO_2 film was carried out in two steps. In the first step, a loose layer of SiO_2 from a spirit lamp flame was deposited on the thermocouple. In the second step, the deposited layer was sintered in a burner flame at the melting point of quartz. As a result, the thermocouple was covered with a thin layer of SiO_2 melt. The resulting coating was stable in the investigated flame. The stability of the coating is confirmed by the fact that in flame temperature measurements with the same thermocouple in several experiments, the thermocouple showed the same temperature values. It is known that in the case of destruction of the coating, the measured temperature continuously increases and the thermocouple is gradually destroyed. In our work, the thermocouple remained unchanged after the completion of all experiments. An uncoated thermocouple placed in the flame burned out almost instantaneously. One of the thermocouples (TC1) had a circular cross section with a diameter of ~24 μm. The other two thermocouples had rectangular cross sections, and their dimensions were 10 × 110 μm (TC2) and 20 × 125 μm (TC3), including the layer of coating. The length of the thermocouple's shoulders was ~10 mm. This corresponds to length-to-diameter ratios above 400, which [4,12] provides minimum conduction errors and indicates that heat loss by conduction to the supports are negligible. The thermocouple junction was placed near the center of the flame. A stretching device, shown in Fig. 1, for the lead wires of the thermocouple [16], provided parallel alignment of the thermocouple relative to the top of the burner. In addition, the stretching device prevented deformation of ribbon thermocouples in a flame. During temperature measurements, the distance between the thermocouple junction and the burner was controlled using a cathetometer with as accuracy of up to 0.01 mm. The error of the thermocouple measurements was within ±30 K. Experimental uncertainty is determined from the scatter from 4 to 5 repeated measurements of a temperature profile.

3. Numerical simulation of the flow

The external planar flow field over a thermocouple inserted in the flow at some distance from the burner was simulated using the full set of unsteady Navier–Stokes equations. A finite-difference representation of the governing equations was made on a staggered grid, which facilitated the development of an effective algorithm for simulating viscous flows [17]. An approximate allowance for the heat release due to chemical reactions was made by

adding a source term (Q) to the energy equation to provide a given temperature distribution in the unperturbed isobaric flame, i.e., with no thermocouple in the flame. Numerous test simulations confirm that the solution of the finite-difference relations is equivalent to the solution of the governing differential equations.

The simulations were performed for the flow of the burner-stabilized premixed methane–oxygen–argon flame (initial composition 6%CH_4 + 15%O_2 + 79%Ar) studied in our experiments. The combustible gas mixture was assumed to be a single-component perfect gas with a molecular weight of 37.32 kg/kmole and a specific heat ratio $\kappa = 1.5747$ calculated from the parameters of the real gas mixture at the burner surface. The temperature dependence of the dynamic viscosity μ of the gas was described by the Lennard–Jones (6–12) potential with parameters $\sigma = 3.418$ Å and $\varepsilon/k = 124$ K typical of argon [18]. Since the main component of the mixture is argon, the Prandtl number ($\mathrm{Pr} = \mu C_p/\lambda$, $C_p = \kappa R/(\kappa - 1)$ is specific heat at constant pressure, R is the gas constant, λ is the thermal conductivity) was set to that for argon, i.e., $\mathrm{Pr} = 2/3$. For the numerical solution, the density ρ, pressure p, and temperature T were normalized by the corresponding parameters at the burner (denoted below by the lower subscript 0), and the transverse (u) and longitudinal (w) velocity components were normalized by the speed of sound, $c_0 = 359.3$ m/s. The spatial variables x and y were conveniently expressed in mm.

The above-mentioned source term (Q) in the energy equation was obtained from the following relation representing the condition for steady solution of energy equation, written in non-dimensional form:

$$\frac{\partial T}{\partial t} = Q_{\mathrm{conv}} + Q_{\mathrm{vis}} + Q = 0, \tag{1}$$

where the convective terms in the energy equation are denoted by Q_{conv} and the viscous terms by Q_{vis}. The finite-difference representation of relation (1) for one-dimensional flow was performed on the same staggered grid for the axial coordinate as in two-dimensional calculations below, with the source term being defined at the center of the cell. The temperature distribution in the flow was set in accordance with the results of simulating the undisturbed flame flow with the CHEMKIN PREMIX code [13]. The distributions of the density and axial velocity in relation (1) were found from the continuity equation and the equation of state, assuming the pressure to be constant and equal to 760 torr. For the source term to be consistent with the flow model considered, we neglected small changes in the mean molecular weight, occurring in the real undisturbed flame due to chemical reactions. The dependence of $Q(x)$ have a sharp maximum at $x = 0.5$ mm, which reflects heat release in the unperturbed methane flame under the conditions considered. Together with the approach using spatially fixed sources $Q(x)$, we employed another source term, namely, $Q(T)$, which provides a more detailed description of the non-linear interaction between chemical and gas dynamical processes. Due to the dependence $T(x, y)$, the source term $Q(T)$ also depends on x and y. The unperturbed flame is well reproduced by both of these approaches.

The dependence of $Q(T)$ is given in Fig. 2. Small values of Q at low temperatures (near the burner) reflect the predominant effect of thermal conductivity on the temperature profile in this region of the flame front. To convert the source term on the right side of the energy equation to dimensional form (in units of power/volume), the values shown in Fig. 2 should be multiplied by $(e_0 c_0 \rho(T)/h_0)$, where $e_0 = RT_0/(\kappa - 1)$ is the specific internal energy at the burner surface, $\rho(T)$ is the dimensional density in the undisturbed flame, and $h_0 = 1$ mm is the used unit of linear variables. Thus, at $T = 1465$ K, where the source term reaches the maximum non-dimensional value of 0.03676 (see Fig. 2), the corresponding dimensional value is 0.0159 W/m^3.

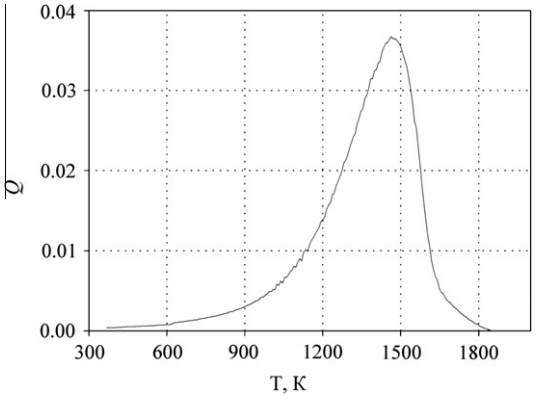

Fig. 2. Source term $Q(T)$ in non-dimensional form for the energy Eq. (1). For the conversion of the source term to a dimensional form (in power/volume), see the text.

The simulation domain was a rectangle with dimensions of 2.4 mm in the longitudinal direction (x) and 1.5 mm in the transverse direction (y) with mesh sizes of the grid $dx = dy = 2.5$ μm. Boundary conditions for the flow were specified as follows. At the burner's surface (left boundary), the conditions for all quantities were imposed based on the solution for the unperturbed isobaric flame obtained using PREMIX code [13] for the mixture considered ($T = 368$ K, $w = 15.68$ cm/s, $u = 0$). At the right boundary, both velocity components and temperature were specified by interpolation from internal points of the domain, and the pressure on this surface was prescribed to be constant (isobaric flame). In the plane of symmetry (lower boundary through the middle of the thermocouple), the transverse velocity and the transverse derivatives of the longitudinal velocity and temperature were set equal to zero. In order to avoid problems with boundary conditions at the upper boundary, the latter was also treated as a plane of symmetry, which is equivalent to assuming that we have an infinite row of thermocouples placed at the same distance from the burner. The step of this row, i.e., the distance between the middle points of neighboring thermocouples, was chosen to be large enough to minimize the distortion of the flow field caused by this assumption. At the surface of the thermocouple, the normal velocity component was set equal to zero and the tangential velocity component was specified with the velocity slip taken into account [17], although the slip is very small under the conditions used.

Estimates showed that, due to the high conductivity of the metallic thermocouple, the temperature change within the thermocouple could be neglected and the temperature was therefore assumed to be uniformly distributed over the thermocouple's surface. This surface temperature was determined from assuming the heat flux to the surface from the gas is equal to the radiative heat flux from the surface for the assumed value of the emissivity ε (for $\varepsilon = 0$, the surface is under adiabatic conditions). At each computational time step, the thermocouple's temperature was iteratively calculated to satisfy the above condition. It should be noted that the approach described here gives a temperature for the thermocouple, which can be directly compared with measurements, without applying semi-empirical corrections for radiation loss.

The steady flow fields for the complete set of values for the determining parameters (the value of ε, the model for the source term Q, the distance of the thermocouple from the burner) were calculated for ribbon thermocouple TC3, and these calculation results will be discussed in detail below. Some values were calculated for thermocouples TC1 and TC2. The main features of the perturbed flow due to the thermocouple's presence were found to be qualitatively similar for all the thermocouples considered.

4. Results and discussion

A methane flame was chosen for this study because the mechanism of chemical reactions in this flame is fairly well known. The temperature profile in the flame can be predicted with appropriate accuracy using the GRI 3.0 mechanism [19] for methane oxidation and the PREMIX code. This mechanism reproduces a large number of various measurements, including data on the burning velocity and structure of methane flames.

Figure 3 shows the unperturbed temperature profile T_{up} calculated using the PREMIX code (curve 1) and the results of four temperature profile measurements in the methane flame using thermocouple TC3 (curve 2), without a correction for radiation. We could not measure the temperature at distances from the burner surface smaller than 0.1 mm. Moreover, there is the problem of flame-front formation by a burner in the form of a porous disc, which requires a separate investigation.

In the temperature range from approximately 800 to 1100 K, the measured temperatures are higher than the unperturbed flame temperature, despite heat loss due to radiation. The data scatter for TC3 (as well as for TC1 and TC2) was approximately ±10 μm on the x axis and ± (15–20 K) on the T axis.

Smoothed temperature profiles obtained by the three types of thermocouple with a correction for radiation applied are presented in Fig. 4. The correction for heat loss due to radiation was calculated by the formula [9] for the case of a circular thermocouple, with the equivalent diameter of the ribbon thermocouple determined as the ratio of the thermocouple cross-sectional perimeter to π [20]. The temperature dependence of the emissivity ε of the thermocouple coated with SiO_2 was taken into account. For fused quartz, this dependence [21] can be approximated by

$$\varepsilon(T) = 0.163297 + 0.766332/(1 + \exp((T - 583.467752)/146.53391))^{0.317496} \quad (2)$$

with the temperature T expressed in K. This relation was determined by approximating experimental data in the temperature range from 300 to 1700 K.

At distances of about 0.2–0.4 mm from the burner, where the temperature varies from 800 to 1300 K, the measured temperatures exceed the unperturbed ones: at a distance of 0.3 mm, the excess is about 125 K. This excess is greater than the measurement errors. Similar effects were observed in all the experiments performed.

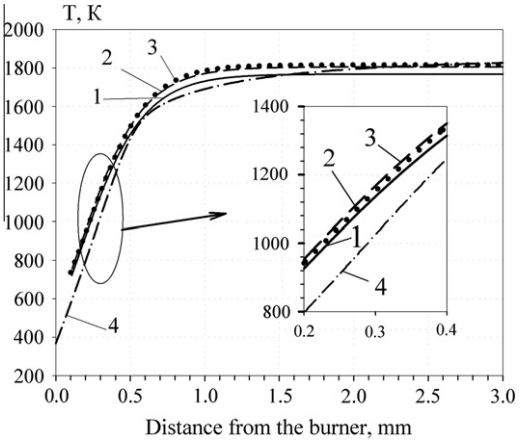

Fig. 4. Temperature profiles in the methane flame. Curves 1–3: smoothed experimental temperature profiles with correction for radiation heat loss, 1 – T_{TC1}, 2 – T_{TC2}, 3 – T_{TC3}. Curve 4 – T_{up}. The fragment on the right shows in more detail the excess of the measured temperature over the temperature of the unperturbed flame.

For a more detailed analysis of the measured temperature profiles, Fig. 5 shows the difference between the thermocouple readings corrected for radiation loss and the unperturbed flame temperature ($\Delta T = T_{TCi} - T_{up}$) for all thermocouples TCi (i = 1–3). As can be seen from Fig. 5 (curves 1–3), the temperature elevation (ΔT) profiles have two maxima, the first of which is at 0.2 mm from the burner and has $\Delta T \sim 125$–150 K. The second elevation, with a maximum value of 40–100 K is at 0.9 mm from the burner. We assume that the first temperature maximum is related to the gas deceleration near the thermocouple and the presence of a temperature gradient in the flame. This assumption will be confirmed below by numerical simulation.

The second maximum temperature rise is presumably related to catalytically-induced heating due to the recombination of radicals on the thermocouple. Fig. 5 also shows concentration profiles of H and OH radicals in the unperturbed flame calculated using the PREMIX code [13]. It can be seen that the positions of the H and OH concentration maxima are in good agreement with the position of the second maximum of the temperature elevation. The effect of radical recombination on the thermocouple was quantitatively

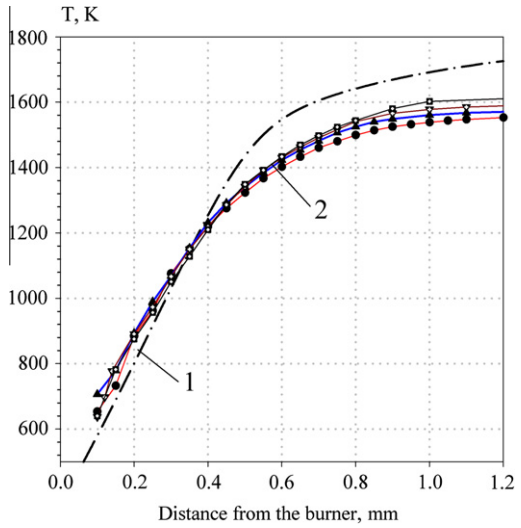

Fig. 3. Temperature profiles in the methane flame. 1: T_{up} (unperturbed flame, PREMIX), 2: raw measurements: T_{TC3} profiles without a correction for radiative heat loss.

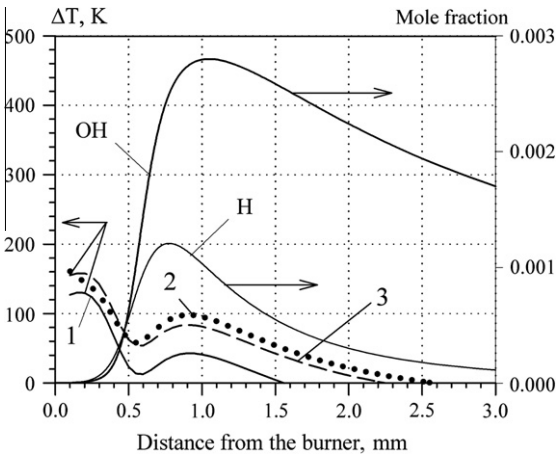

Fig. 5. Thermocouple-measured temperature elevation above the unperturbed flame temperature (curves 1–3), 1 – ($T_{TC1} - T_{up}$), 2 – ($T_{TC2} - T_{up}$), 3 – ($T_{TC3} - T_{up}$). H and OH are radical concentration profiles in the unperturbed flame.

estimated as follows. The number of radical collisions (N) per unit thermocouple surface per unit time was calculated from the H and OH concentration profiles. The heat flux to the thermocouple was obtained using the known values of heat release (H^*) in a single recombination event on the surface. A similar approach to accounting for heat release on the thermocouple due to the recombination of H radicals on this surface has been described before [5]. The heat flux data were transformed to temperature data by the procedure used above to calculate the radiative correction [9]:

$$\Delta T = T_c - T_g = [1.24 d^{3/4} K N H^* (\mu/\rho w)^{1/4}]/\lambda \qquad (3)$$

where T_c is the temperature of the thermocouple junction, T_g is the gas temperature, d is the thermocouple's diameter, and K is the probability of radical recombination. The temperature dependencies of λ and μ were the same as those used in simulating the gas flow. The results were as follows: in order that the observed second maximum temperature rise (see Fig. 5) may be explained by radical recombination, the probability of recombination per collision must be in the range from 10^{-3} to 10^{-2}, which seems quite realistic [22] for the anti-catalytic SiO_2 used. It is interesting to note that the probability of radical recombination on a purely metallic thermocouple surface is close to unity [5]. The negative values in curves 1–3 at large distances are due to the approximate allowance for the radiation correction and do not affect the conclusions.

Figure 6 shows numerical temperature profiles predicted by the model with the source term in the form $Q(T)$ and $Q(x)$ for ribbon thermocouple TC3 with $\varepsilon = 0$ and the temperature profile in the unperturbed flame T_{up}. These data demonstrate that under net conditions, i.e., without energy loss due to radiation, the thermocouple is significantly overheated to above the unperturbed temperature. The profiles illustrate the nature and magnitude of the effect predicted by the model of perturbed flow around a thermocouple placed in the flame front.

For a more detailed analysis of thermocouple-induced temperature perturbations, Fig. 7 shows the deviation of the experimental and numerical temperature profiles for ribbon thermocouple TC3 from the unperturbed data ($\Delta T = T - T_{up}$). The simulation data for the models with $Q(T)$ and $Q(x)$ agree qualitatively with each other, although there is a noticeable quantitative difference between them for both $\varepsilon = 0$ (curves 1 and 2) and $\varepsilon = \varepsilon(T)$ (curves 3 and 4). For $\varepsilon = 0$, the maximum overestimation of the temperature by the thermocouple is ~100 K for the model with $Q(T)$ and 70 K for the model with $Q(x)$ at $x \sim 0.3$–0.4 mm. The data for $\varepsilon = \varepsilon(T)$

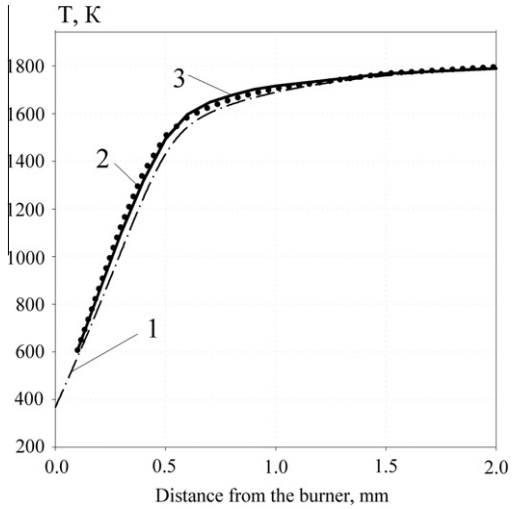

Fig. 6. Unperturbed (curve 1) and numerical (curves 2 and 3) temperature profiles for thermocouple TC3: 1 – T_{up}; 2 – $Q(T)$, $\varepsilon = 0$; 3 – $Q(x)$, $\varepsilon = 0$ (solid line).

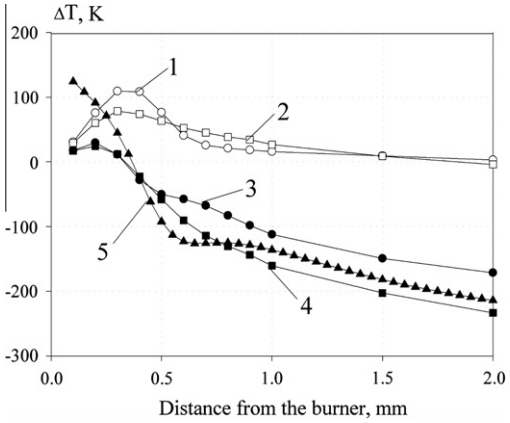

Fig. 7. Deviation of numerical (curves 1–4) and experimental (curve 5) temperature profiles from unperturbed data (1 – $Q(T)$, $\varepsilon = 0$; 2 – $Q(x)$, $\varepsilon = 0$; 3 – $Q(T)$, $\varepsilon = \varepsilon(T)$; 4 – $Q(x)$, $\varepsilon = \varepsilon(T)$).

are negative almost everywhere in the flame region except at small distances from the burner (⩽0.3 mm) due to radiation heat loss from the thermocouple. The experimental data (curve 5) are in qualitative agreement with simulation results. The reason for the significant overestimation of the experimental values at small distances from the burner is not clear. The non-monotonic nature of the experimental profile with the local maximum at $x \sim 0.8$–0.9 mm can be attributed to the additional heating of the thermocouple due to the catalytic recombination of H and OH radicals discussed above (see Fig. 5). In view of this effect, the analysis of curves 3–5 in Fig. 7 leads to the conclusion that the real emissivity ε of the thermocouple coated with SiO_2 should be slightly higher than that used in this study from Eq. (2), at least in the high-temperature range ($T > 1200$ K).

Since the difference ($T(\varepsilon = 0) - T(\varepsilon)$) can be treated as the exact value of the correction factor for heat loss due to radiation for the numerical experiment performed, the simulation allows one to test existing semi-empirical approaches to the correction of the results of thermocouple measurements in flames. In Fig. 8, the corresponding data for the models with $Q(T)$ (curve 1) and with $Q(x)$ (curve 2) are compared with the two approaches recommended by Kaskan [9] and used above (curve 3) and in [20] (curve 4). As can be seen from Fig. 8, the existing semi-empirical data are in good agreement with each other. Despite some differences between the results predicted by the models treating the source term

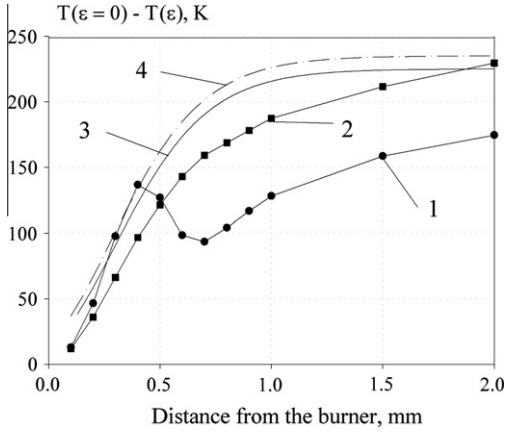

Fig. 8. Numerical (curves 1 and 2), and semi-empirical (curves 3 and 4) data for heat loss from thermocouple TC3 due to radiation (1 – model with $Q(T)$, 2 – model with $Q(x)$, 3 – [9], 4 – [20]).

as $Q(T)$ or $Q(x)$, whose causes require further investigation, both of these models lead to smaller correction factors, indicating more intense heat transfer between the thermocouple and chemically non-equilibrium reactive flow compared to the same process in chemically inert flow usually used in heat transfer experiments [9,20].

Figures 9–11 show the fields of streamlines, longitudinal velocity and isotherm, respectively, obtained for the case of flow around thermocouple TC3 and the region occupied by the thermocouple body whose center is at a distance $x = 400$ μm from the burner for the model with $Q(T)$ and $\varepsilon = 0$. This position of the thermocouple corresponds to the flame zone with the most significant perturbations of the temperature profile by the thermocouple (see curve 1 in Fig. 7). The flow direction in Figs. 9–11 is from left to right.

As can be seen from Fig. 9, which shows the streamlines, the flow is a typical laminar flow around an obstacle (thermocouple). This is not surprising since the Reynolds number determined from the unperturbed flow parameters and the thermocouple width is about 0.4. In the unperturbed flow, i.e., in the absence of a thermocouple, the streamlines are a set of straight lines parallel to the abscissa.

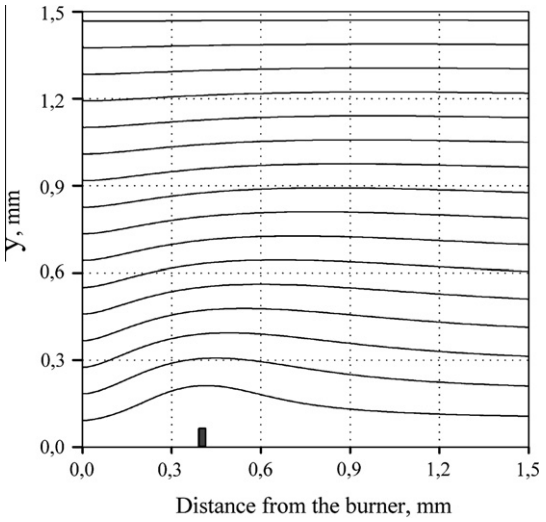

Fig. 9. Streamlines picture for flow around thermocouple TC3 predicted by the model with $Q(T)$ and $\varepsilon = 0$.

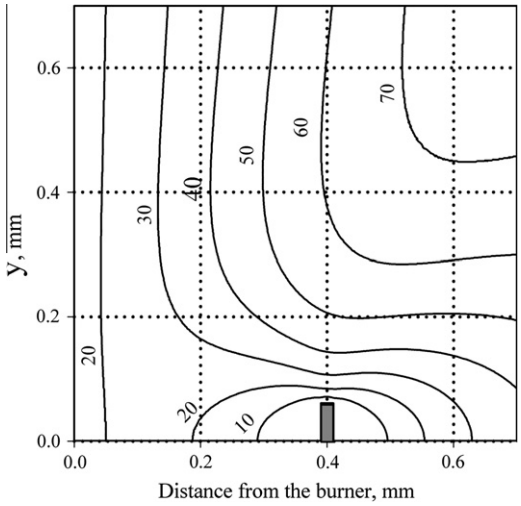

Fig. 10. Longitudinal velocity field (cm/s) for flow around thermocouple TC3 for the same conditions as in Fig. 9.

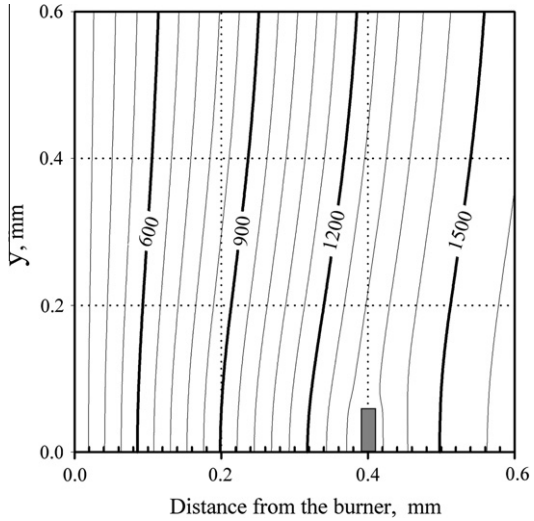

Fig. 11. Field of isotherms (K) for flow around thermocouple TC3 for the same conditions as in Fig. 9.

An analysis of the longitudinal velocity field (Fig. 10) shows that at $y = 0$ the velocity of the flow directed to the central part of the thermocouple, containing the thermocouple junction, decreases from ~20 cm/s ($x \sim 200$ μm) to nearly zero as the thermocouple is approached, and downstream of the thermocouple, it increases slowly. One can see that at a distance of ~200 μm behind the thermocouple, the flow velocity is about 26 cm/s. This value is much lower than the velocity in the unperturbed flame at a distance $x = 400$ μm from the burner (~60 cm/s). Thus, the region of distortion of the longitudinal velocity field is about 250 μm in front of and behind the thermocouple. The dimension of the perturbed region (~500 μm) is more than 20 times larger than the thermocouple thickness and is almost half the width of the flame considered.

Thus, the thermocouple forms a deceleration zone in the gas flow and, at the same time, it reflects the temperature inside this perturbed region. Since the thermocouple is placed in the gas flow with intense heat release due to chemical reactions, the flow deceleration by the thermocouple leads to additional heat release and, hence, to distortion of the field of isotherms (see Fig. 11) at the thermocouple. As a result, the temperature at the thermocouple is higher than the unperturbed flame temperature and, consequently, the thermocouple readings overestimate unperturbed temperature values. For the methane flame considered, this overestimation depends on the thermocouple's shape and position and is limited to a value of about 100 K (see Figs. 7 and 11). For flames with higher pressure and higher gas velocities, such as flames of condensed systems [15], this effect should be even more significant although the perturbation of such flames by thermocouples requires special consideration.

5. Conclusions

The results can be summarized as follows:

1. The temperature profiles in the methane flame, as measured by thermocouples and corrected for radiation loss, were found to be consistently higher than those calculated by CHEMKIN in the unperturbed flame, where the temperature gradient was high and in the region with maximum concentrations of the radicals H and OH.
2. The model developed for a perturbed flow around a thermocouple in a flame, based on the Navier–Stokes equations with a source term added to the energy equation, showed that where

the temperature gradient was large, the observed effect may be caused by a deceleration of the flow just before the thermocouple, resulting in an additional heat flux to the thermocouple, due to chemical reactions.

3. The estimations show that, in the region with maximum concentrations of H and OH radicals, the observed effect can be attributed to the catalytic recombination of these flame radicals on the thermocouple, in spite of the fact that the thermocouple is coated with an anti-catalytic layer of SiO_2.
4. The model developed for perturbed flow around a thermocouple predicts more intense heat transfer between the thermocouple and chemically non-equilibrium reacting flow than in a similar situation for a chemically inert flow.
5. These flow perturbations due to thermocouples seem to be important and should be taken into account when interpreting measurements of temperature along a flame using a thermocouple.

References

[1] R.M. Fristrom, A.A. Westenberg, Flame Structure, McGraw-Hill, New York, 1965.
[2] Ya B. Zel'dovich, G.I. Barenblatt, V.B. Librovich, G.M. Makhviladze, The Mathematical Theory of Combustion and Explosion, Consultants Bureau, New York, 1985.
[3] J. Warnatz, U. Maas, R.W. Dibble, Combustion, Physical and Chemical Fundamentals, Modeling and Simulations, Experiments, Pollutant Formation, third ed., Springer, Berlin, 2001.
[4] A.A. Zenin, S.V. Finjakov, Comb. Explos. Shock Waves 45 (5) (2009) 559–578.
[5] A.N. Hayhurst, D.B. Kittelson, Combust. Flame 28 (1977) 301–317.
[6] O.P. Korobeinichev, A.A. Paletskii, E.N. Volkov, Russ. J. Phys. Chem. B 2 (2) (2008) 206–228.
[7] R. Pain, Combust. Explos. Shock Waves 36 (1) (2000) 21–28.
[8] A.A. Zenin, Prog. Astronaut. Aeronaut. 143 (1992) 197–231.
[9] W.E. Kaskan, Proc. Combust. Inst. 6 (1957) 134.
[10] C.R. Shaddix, Correcting thermocouple measurements for radiation loss: a critical review, in: Proc. 33rd National Heat Transfer Conference, August 15–17, Albuquerque, New Mexico, 1999.
[11] A.A. Zenin, J. Prop. Power 11 (4) (1995) 752–759.
[12] M.V. Heitor, A.L.N. Moreira, Prog. Energy Combust. Sci. 19 (1993) 259–278.
[13] R.J. Kee, J.F. Grcar, M.D. Smooke, J.A. Miller, A Program for Modeling Steady, Laminar, One-Dimensional Premixed Flames, Report No. SAND85-8240, Sandia National Laboratories, 1985.
[14] N. Bahlawane, U. Struckmeier, T.S. Kasper, P. Obwald, Rev. Sci. Instrum. 78 (2007) 013905.
[15] M.W. Beckstead, Comb. Explos. Shock Waves 43 (2) (2007) 134–136.
[16] O.P. Korobeinichev et al., Comb. Sci. Technol. 116 (1) (1996) 51–67.
[17] A. Broc, S. De Benedictis, G. Dilecce, M. Vigliotti, R.G. Sharafutdinov, P.A. Skovorodko, J. Fluid Mech. 500 (2004) 211–237.
[18] J.O. Hirschfelder, Ch.F. Curtiss, R.B. Bird, Molecular Theory of Gases and Liquids, Wiley, New York, 1954.
[19] G.P. Smith, D.M. Golden, M. Frenklach, N.W. Moriarty, B. Eiteneer, M. Goldenberg, C.T. Bowman, R.K. Hanson, S. Song, W.C. Gardiner, Jr., V.V. Lissianski, Z. Qin. <http://www.me.berkeley.edu/gri_mech/>.
[20] H.Y. Wong, Handbook of Essential Formulae and Data on Heat Transfer for Engineers, Longman, London; New York, 1977.
[21] Yu V. Polezhaev, F.B. Yurevich, Heat Protection, Energiya, Moscow, 1976 (in Russian).
[22] N.M. Rubtsov, G.I. Tsvetkov, V.I. Chernysh, Russ. J. Phys. Chem. A 83 (10) (2009) 1701–1704.